MULTIPLE MENKES COPPER ATPASE (ATP7A) TRANSCRIPT AND PROTEIN VARIANTS ARE INDUCED BY IRON DEFICIENCY IN RAT DOUDENAL ENTEROCYTES

Yan Lu[a], **Changae Kim**[a], and **James F. Collins**[a,*]

[a]Food Science & Human Nutrition Department, University of Florida, Gainesville, FL. USA

Abstract

The Menkes copper ATPase (Atp7a) pumps copper into the *trans*-Golgi for cuproenzyme synthesis, and translocates to the basolateral membrane of enterocytes for copper export. Recent studies demonstrated that three 5' end splice variants of the Atp7a transcript exist in rat duodenum, all of which are strongly induced during iron deprivation. To explore a possible role for Atp7a (and copper) in intestinal iron absorption, the current studies were undertaken to test the hypothesis that multiple Atp7a transcript and protein variants exist in intestinal epithelial cells. Northern blot analyses using probes generated from the full-length Atp7a cDNA revealed several specific hybridization bands, all of which were more intense in RNA samples extracted from duodenal enterocytes isolated from iron-deficient rats. A PCR-based approach, using forward primers specific for the alternative 5' end splice variants and a reverse primer in exon 23, demonstrated that 3 full-length transcripts exist in rat IEC-6 cells. To identify possible Atp7a protein variants, three distinct polyclonal antisera were utilized. The specificity of the antisera was first established by western blotting and immunoprecipitation studies using samples derived from isolated rat enterocytes and Atp7a knockdown IEC-6 cells. Several specific immunoreactive bands were documented, and a unique Atp7a protein distribution in cytosolic vesicle-like structures was noted. In conclusion, multiple Atp7a transcript and protein variants exist in rodent intestinal epithelial cells and are induced by dietary iron deprivation. Further studies will be designed to determine the subcellular distribution of Atp7a protein variants and possible unique functions of each.

Keywords

iron-deficiency anemia; iron; copper; intestine

Introduction

Menke's copper ATPase (Atp7a) is a widely expressed copper transporter that is important for intestinal copper absorption. Under basal conditions, Atp7a is localized to the *trans*-golgi apparatus of enterocytes where it provides copper to newly synthesized cupro-proteins. However, when intracellular copper is elevated, Atp7a translocates to the basolateral

*Corresponding author: J. F. Collins; FSHN Dept., University of Florida, FSHN Bldg., #441, Newell Dr., PO Box 110370, Gainesville, FL, 32611, USA. jfcollins@ufl.edu.

membrane and facilitates copper export into the blood stream. Mutations in ATP7A lead to Menke's disease in humans, which is characterized by intestinal copper accumulation and systemic copper deficiency.

Previously, induction of Atp7a mRNA and protein expression was noted in rodent enterocytes during iron deficiency along with increased copper transport and liver copper accumulation [1, 2]. Subsequently, an *in vitro* model (i.e. IEC-6 cells) was developed to further investigate the molecular mechanism underlying this observation. Actinomycin D inhibition of Atp7a mRNA induction suggested that this process was transcriptionally mediated. Thus, 5' rapid amplification of cDNA ends (5' RACE) was conducted to begin initial characterization of the gene promoter, and unexpectedly, three different 5' end splice variants were identified: one contained exons 1, 1A (a newly discovered exon), 2 and 3; the second contained exons 1, 2 and 3; and the third had exon 1 spliced to exon 3. All of these variants were strongly induced during iron deficiency [3].

To further examine the potential role of Atp7a in intestinal iron homeostasis, the present investigation was undertaken to identify Atp7a transcript and protein variants in rat enterocytes and IEC-6 cells and to quantify their expression during dietary iron deprivation. Northern blot and RT-PCR-based approaches were utilized to identify transcript variants while three different anti-Atp7a antibodies were utilized to identify protein variants. The data presented herein supports the existence of multiple splice and immunoreactive protein variants in intestinal epithelial cells, many of which are strongly induced during iron deficiency.

Methods

IEC cells were obtained from ATCC and maintained at 37° C in a humidified incubator with 5% CO_2 in high glucose DMEM medium supplemented with 10% fetal bovine serum, 1% penicillin/streptomycin solution and 0.1% insulin (Sigma). The cells were used between passages ~18–25.

Three gene-specific shRNA entry vectors (BLOCK-iT) targeting the rat Atp7a transcript (GenBank accession # NM_052803) were designed and produced by Invitrogen. The shRNAs were designed to hybridize to regions of the mRNA near bps 1145, 1800 and 3599 (from the 5' end). The shRNA plasmids were stably transfected into IEC-6 cells by antibiotic selection essentially according to the manufacturer's instructions. Trial experiments determined that cells expressing all three Atp7a-specific shRNAs simultaneously showed more significant inhibitory effects than individual shRNA expressing cells. Thus, cells transfected with all three shRNA vectors (called "mix") were used for all experiments along with negative control shRNA (Invitrogen) transfected cells (called "[−]").

All animal studies were approved by the University of Florida IACUC. Weanling, male Sprague-Dawley rats (Harlan, Indianapolis, IN) were housed in overhanging, wire mesh-bottom cages for 35 days until sacrifice. The rats had food and iron-free water *ad libitum*. The diets were based on the AIN-93G formulation (Dyets Inc., Bethlehem, PA) with ~200 ppm Fe (control; Ctrl) or ~3 ppm Fe (iron deficient; FeD). Although the AIN-93G formulation includes 40 ppm iron, the authors have used this control diet modeled after standard rodent chows (with ~200 ppm Fe) for several years. This diet is not considered a "high iron" diet, since the animals show no adverse affects (as is also noted with rodents on standard chow) and further, the iron is present in a less bioavailable form in the diet (ferric citrate). Except for iron levels, the diets were otherwise identical. Previous protocols were followed for tissue collection and enterocyte isolation [4].

Confluent IEC-6 cells and isolated enterocytes were processed into cytosol and membrane fractions as previously described [5] or lysed by hypotonic buffer plus 0.25% (v/v) NP-40 to obtain total cellular protein devoid of nuclear protein (called "cell extract").

Total RNA was extracted from IEC-6 cells or rat enterocytes using TRIzol reagent (Invitrogen). Five μg of total RNA was converted to cDNA by SuperScript III first-strand cDNA synthesis system (Invitrogen) following the manufacturer's recommendations. To amplify full-length Atp7a transcripts, gene-specific primers were designed to span two different 5' exons, and the single reverse primer was within exon 23. The following forward primers were used: exon 1/1A, 5'-tggaatcctagacagaatctactat-3'; exon 1/2, 5'-cctggaatcctaggaatgtaaagaca-3'; exon 1/3, 5'-cctggaatcctacctttccctagaa-3'. The reverse primer in exon 23 was as follows: 5'-acataatgccaggttcagagctcc-3'. PCR was accomplished using Ex *Taq* DNA polymerase (Takara), essentially according to the manufacturer's instructions, using standard amplification conditions.

Total RNA was isolated from IEC-6 cells or rat enterocytes and loaded onto denaturing 1% agarose gels for separation and verification of integrity. RNA was subsequently transferred onto nylon membranes and cross-linked under UV light. The full length Atp7a cDNA (containing exons 1–23) was amplified by RT-PCR, cloned into a plasmid vector and verified by sequencing. The cDNA insert was subsequently excised from the vector, gel purified and biotin-labeled DNA probes were generated (DIG High Prime DNA labeling and Detection Starter Kit II, Roche). Blots were hybridized and otherwise processed under high stringency conditions, according to the manufacturer's instructions.

One hundred μg protein samples (cytosol, membrane or cell extract) were mixed with 1 μl of antibody in binding buffer (25 mM Tris-HCl, 140 mM NaCl, pH 7.4) in the presence of 1% NP-40 in a 300 μl reaction overnight at 4° C. Then, 30 μl of 50% (v/v) protein A sepharose (Sigma) was added to the mixture and the sample was mixed for 60 min at 4° C. The sepharose beads were next pelleted at 2,500 *g* for 3 min. Supernatants were removed and the pellets were washed with 25 mM Tris-HCl, 500 mM NaCl, pH 7.4 buffer 3 times. Thirty μl binding buffer and 10 μl 4X sample loading buffer were added to the final pellets, which were then heated at 78° C for 15 min to release the protein-antibody complex bound to the protein A sepharose. For blocking experiments, Ab was premixed with 2 volumes of antigenic peptide(s) in a 10 μl 1X PBS mixture and incubated for 2 hrs at room temp with occasional gentle mixing or overnight at 4° C. A control reaction with the same volume of Ab in 1X PBS (minus the peptide[s]) was processed identically.

Thirty μg protein samples or 35 μl of the eluants from IP experiments were loaded onto 7.5% SDS/PAGE gels for electrophoretic separation. Proteins were transferred to PVDF membranes and reacted with different anti-Atp7a antibodies, by standard methods [3]. One Atp7a antibody (called 54–10) was a polyclonal anti-serum from rabbits that were injected with two peptides (NH_2-pkkdrsanhldhkre-COOH and NH_2-khsllvgdfredddttl-COOH); this reagent has been extensively validated [1, 3, 4]. Atp7a "Long" antibody was generated by injecting one 37 amino acid peptide from the N-terminal region (NH_2-rtieqqigkvngvhhikvsleeksatviynpklqtpk-COOH) into two rabbits; the reagent used herein was the affinity-purified product (Open Biosystems, Huntsville, AL). A well-validated Atp7a (R17) antibody was a kind gift from Dr. Julian Mercer, Australia. This antibody was raised in sheep against the 590 N-terminal region of Atp7a containing the six Cu-binding domains fused to a $(His)_6$-tag at the N-terminus [6]. HRP-conjugated anti-rabbit and anti-sheep secondary antibodies were from Bethyl laboratories. For Ab blocking experiments, Ab was mixed with peptides as mentioned in the IP section prior to adding it to the blocking buffer (5% non-fat dry milk in 1X TBST).

IEC-6 cells were seeded onto poly-D-lysine coated coverslips in 6-well cell culture plates. The detailed protocols are described elsewhere [7]. "Long" Ab and an Alexa Fluor 647 secondary antibody (Invitrogen) were used at a 1:1000 dilution along with confocal microscopic imaging.

Results and discussion

The iron status of rats was determined by measuring hemoglobin (Hb) and hematocrit (Hct) levels in blood removed at sacrifice. Significantly decreased Hb and Hct (>60%) was observed in all rats consuming the FeD diet (data not shown), consistent with previously published studies [2, 5, 8].

Northern blot analysis of RNA extracted from duodenal enterocytes of Ctrl and FeD rats using biotin-labeled full length Atp7a-specific cDNA probes revealed at least four transcripts (Fig. 1A). Moreover, all transcripts were induced upon iron deprivation. This supports previous investigations which documented transcriptional regulation of Atp7a [9] and induction during iron deprivation [2, 3]. To date, to our knowledge, this is the first study that used the entire Atp7a cDNA sequence (exons 1–23; >4 kb) as a template to generate probes for Northern blot analysis. The exact nature of the different bands is not known; however, the band at ~4.3 kb could represent the "full-length" Atp7a transcript, as this size is consistent with the longest cDNA clone deposited in GenBank (accession # NM_052803). Previously, Reddy et al. [10] used a 530 bp oligonucleotide homologous to exon 23 as a probe and identified only one hybridization band at ~5.5 kb in human cells. Moreover, Ackland et al. [11], generated probes from the "N-terminal" region of the Atp7a transcript and reported a single hybridization band at ~8.5 kb in human breast cancer cells. In the current study, full-length Atp7a probes also hybridized with transcripts in RNA isolated from rat IEC-6 cells (Fig. 2B). Longer gel runs revealed that the major hybridization band at ~4.3 kb was actually a doublet, possibly revealing putative splice variants of very similar size. Furthermore, consistent with the Northern blot data, multiple, potential alternative splice variants were noted by RT-PCR using exon 1 forward and exon 23 reverse PCR primers (Fig. 1C).

Previously, three distinct Atp7a splice variants were identified by 5' RACE [3]. Since the stop codon in the Atp7a cDNA is in the 3' most exon (i.e. #23), a PCR-based approach was utilized to determine if the 5' end splice variants were conjoined with exon 23 in multiple "full-length" transcripts. Forward primers were thus designed to span combinations of 5' exons (i.e. exon 1/1A, 1/2, and 1/3), while a single reverse primer was specific for exon 23. A ~4.6 kb band was amplified using all three primer combinations (Fig. 2A), demonstrating the existence of alternative transcripts. The exon 1/1A and 1/2 splice variants would presumably be translated from a start codon in exon 2, whereas the exon 1/3 splice variant would use an alternative, in-frame start codon in exon 3 [3]. Since multiple Atp7a transcript variants were identified in rat enterocytes and IEC-6 cells, the next objective was to investigate whether Atp7a protein variants existed as well. This issue was addressed using three anti-Atp7a antisera and an array of immunochemical techniques. First, the validity and specificity of the antibodies was assessed by immunoprecipitation (IP) studies combined with western blot analysis. Immunoreactive proteins of similar m.w. were detected by all 3 reagents on western blots (Fig. 3, all panels, left most lanes), and in most cases, more than one band was present. The specificity of the 54–10 antiserum was shown by IP with and without pre-incubation with the immunogenic peptides followed by immunoblotting (Fig. 3A). IP with the Long and R17 antisera also pulled down a protein that was recognized by the 54–10 antiserum, at a consistent m.w. as by western blot (Fig 3C). The Long antiserum revealed a protein of consistent m.w. by IP followed by immunblotting and by western blot alone (Fig. 3B). Lastly, IP with all 3 antisera pulled down proteins recognized by the R17

reagent. All-in-all, these experiments suggest that all three of these reagents are specific for the Atp7a protein in IEC-6 cell extract and membrane preps.

To further address the specificity of these reagents for the rat Atp7a protein, shRNA knockdown cells were established. Quantitative RT-PCR demonstrated that IEC-6 cells expressing a combination of three Atp7a-specific shRNAs showed a significant reduction in Atp7a transcript levels (>50%), as compared to cells expressing a negative control shRNA (data not shown). Immunoblot analysis using all three antisera showed that the Atp7a shRNAs significantly reduced levels of a potential full-size (~190 kDa) Atp7a protein (Fig. 4A and B), providing strong evidence of specificity. Furthermore, the Long antiserum detected multiple immunoreactive bands, all of which were attenuated in Atp7a shRNA expressing cells (F.g 4C). Multiple bands could also be attenuated by pre-incubation of the Long antiserum with the immunogenic peptide (F.g 4D). These experiments prove specificity of the different antisera for the Atp7a protein and provide strong evidence supporting the existence of multiple protein variants in rat intestinal epithelial cells.

As previous findings indicated that the "full-size" Atp7a protein was induced during iron deficiency, it was important to investigate whether any of these putative protein variants were also induced in the duodenum of iron deficient rats. Thus, cytosol and membrane preps from isolated duodenal enterocytes of Ctrl and FeD rats were reacted with the 54–10, Long and R17 Abs. Multiple immunoreactive bands detected by the 54–10 Ab were greatly induced in iron-deficient rats (Fig. 5A), consistent with previous observations [1]. In a shorter exposure, a doublet was clearly visible, possibly relating to "full-length" Atp7a transcripts with alternative 5' ends discussed above. Moreover, immunoreactive bands detected by the Long and R17 antisera were also increased in the samples derived from iron-deficient rats (Fig. 5B).

Lastly, the intracellular localization of immunoreactive protein(s) detected by the Long antiserum was investigated. It is important to note here that co-localization of Atp7a with a *trans*-Golgi-specific marker was noted previously using the 54–10 antiserum [3]. Using the Long antiserum in immunocytochemistry studies in IEC-6 cells, intracellular staining of widely dispersed vesicle-like structures was noted (Fig. 6). The nature of this intracellular "compartment" is not currently known, but will be the subject of further investigation.

Conclusions

Multiple Atp7a transcripts were detected in IEC-6 cells and rat duodenum, with most showing strong induction by dietary iron deprivation. Several Atp7a protein variants also exist in IEC-6 cells and rat duodenal enterocytes and are induced during iron deficiency. The extensive validation of the immune-reagents used via peptide blocking experiments, IP studies and shRNA-mediated Atp7a knockdown, strengthens and validates these observations. Further studies will address sub-cellular localization and potentially novel iron/copper-related physiologic functions of these Atp7a protein variants.

Acknowledgments

References

1. Ravia JJ, Stephen RM, Ghishan FK, Collins JF. Menkes Copper ATPase (Atp7a) is a novel metal-responsive gene in rat duodenum, and immunoreactive protein is present on brush-border and basolateral membrane domains. J Biol Chem. 2005; 43:36221–36227. [PubMed: 16081413]

2. Collins JF, Franck CA, Kowdley KV, Ghishan FK. Identification of differentially expressed genes in response to dietary iron deprivation in rat duodenum. Am J Physiol Gastrointest Liver Physiol. 2005; 288:G964–G971. [PubMed: 15637178]

3. Collins JF, Hua P, Lu Y, Ranganathan PN. Alternative splicing of the Menkes copper Atpase (Atp7a) transcript in the rat intestinal epithelium. Am J Physiol Gastrointest Liver Physiol. 2009; 297:G695–G707. [PubMed: 19679821]

4. Ranganathan PN, Lu Y, Fuqua BK, Collins JF. Discovery of a cytosolic/soluble ferroxidase in rodent enterocytes. Proc Natl Acad Sci USA. 2012; 190:3564–3569. [PubMed: 22331876]

5. Collins JF, Hu Z, Ranganathan PN, Fang D, Garrick LM, Garrick MD Browne RW. Induction of arachidonate 12-lipoxygenase (Alox15) in intestine of iron-deficient rats correlates with the production of biologically active lipid mediators. Am J Physiol Gastrointest Liver Physiol. 2008; 294:G948–G962. [PubMed: 18258795]

6. Ke BX, Llanos RM, Wright M, Deal Y, Mercer JF. Alteration of copper physiology in mice overexpressing the human Menkes protein ATP7A. Am J Physiol Regul Integr Comp Physiol. 2006; 290:R1460–R1467. [PubMed: 16397091]

7. Ranganathan PN, Lu Y, Fuqua BK, Collins JF. Immunoreactive Hephaestin and ferroxidase activity are present in the cytosolic fraction of rat enterocytes. Biometals. 2012 Feb 17. [Epub ahead of print].

8. Jiang L, Ranganathan P, Lu Y, Kim C, Collins JF. Exploration of the copper-related compensatory response in the Belgrade rat model of genetic iron deficiency. Am J Physiol Gastrointest Liver Physiol. 2011; 301:G877–G886. [PubMed: 21852364]

9. Xie L, Collins JF. Transcriptional regulation of the Menkes copper ATPase (Atp7a) gene by hypoxia-inducible factor (HIF2{alpha}) in intestinal epithelial cells. Am J Physiol Cell Physiol. 2011; 300:C1298–C1305. [PubMed: 21346155]

10. Reddy MC, Harris ED. Multiple transcripts coding for the menkes gene: evidence for alternative splicing of Menkes mRNA. Biochem J. 1998; 334:71–77. [PubMed: 9693104]

11. Ackland ML, Cornish EJ, Paynter JA, Grimes A, Michalczyk A, Mercer JF. Expression of Menkes disease gene in mammary carcinoma cells. Biochem J. 1997; 328:237–243. [PubMed: 9359859]
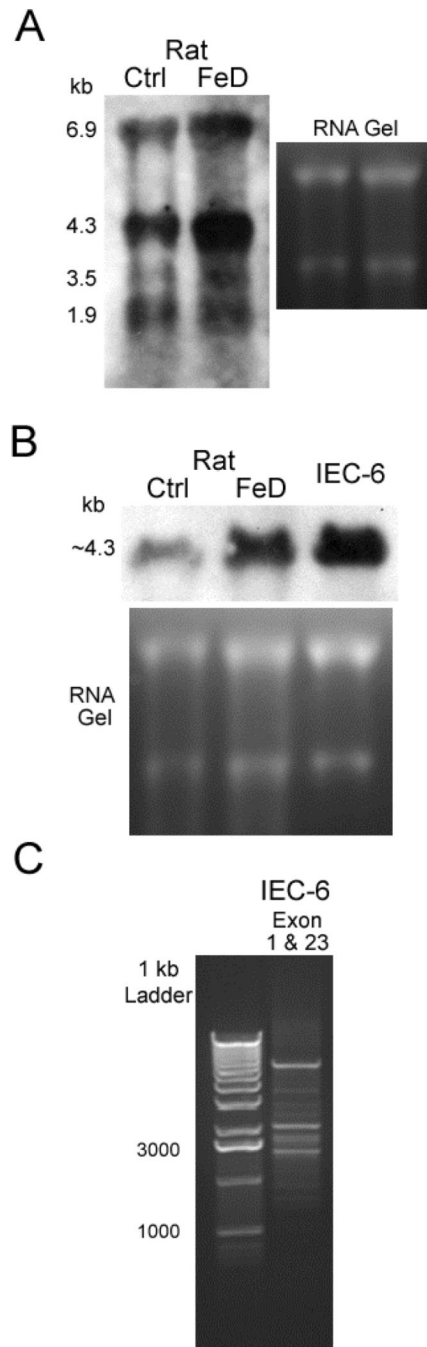
Fig. 1.
Northern blot analysis using full-length cDNA probes with RNA extracted from duodenal enterocytes of Ctrl and FeD rats (**A, B**) and IEC-6 cells (**B**). RNA gels shown in A & B exemplify comparable loading and RNA quality. **C**. RT-PCR amplification of Atp7a cDNA from IEC-6 cells using exon 1 forward and exon 23 reverse primers.
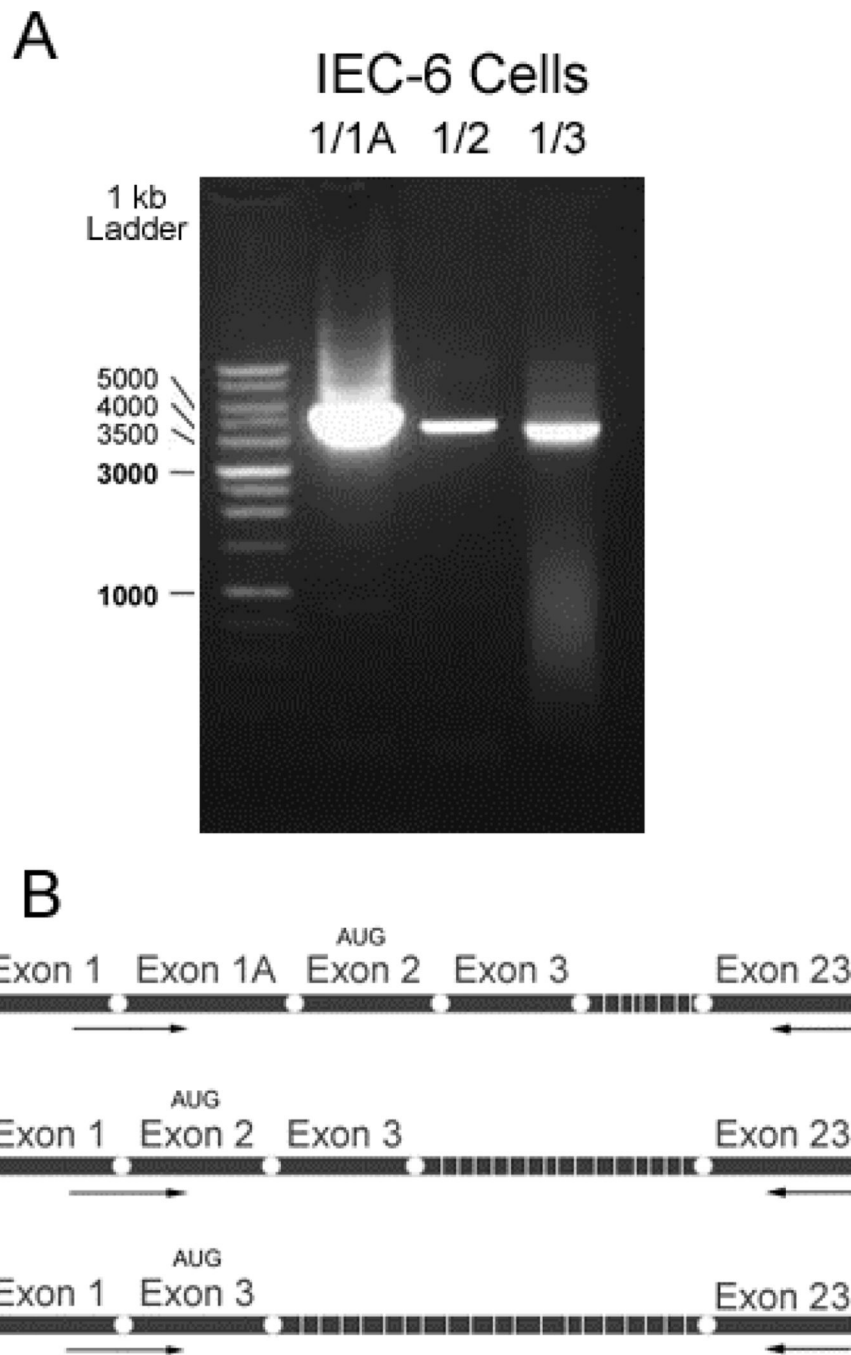
A

IEC-6 Cells

1/1A   1/2   1/3

1 kb
Ladder

5000
4000
3500
3000
1000

B

AUG
Exon 1   Exon 1A   Exon 2   Exon 3   Exon 23

AUG
Exon 1   Exon 2   Exon 3   Exon 23

AUG
Exon 1   Exon 3   Exon 23

Fig. 2.
Full-length Atp7a transcripts were amplified using primers specific for 5' end splice
variants. **A**. PCR amplification of cDNA using different exon-spanning forward and exon 23
reverse primers. **B**. Schematic of three 5' splice variants, with relative locations of primers
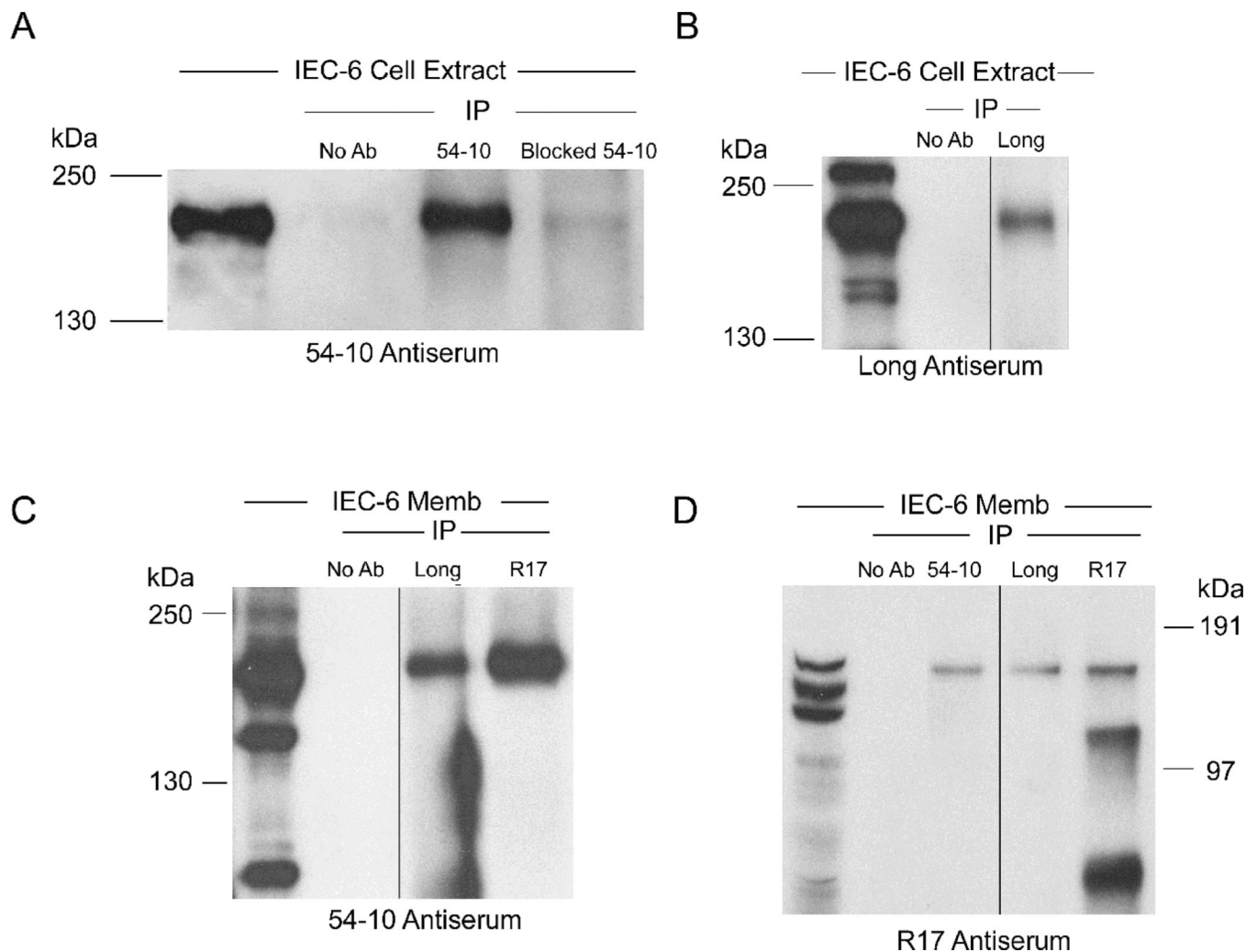noted by arrows.

Fig. 3.
IP of IEC-6 cell extract and membrane preps using three different anti-Atp7a antibodies. **A**. IP by 54–10 or peptide-blocked 54–10 Ab followed by probing with the same Ab; **B**. IP by Long Ab followed by probing with the same Ab; **C**. IP by Long or R17 Ab followed by probing with 54–10 Ab; **D**. IP by 54–10, Long or R17 Abs followed by probing with R17 Ab. In all panels, the left hand most lanes are non IP'd protein samples run as controls. Black lines in B, C & D indicate where nonrelated lanes were removed from images. Memb, membrane. Representative experiments are shown.
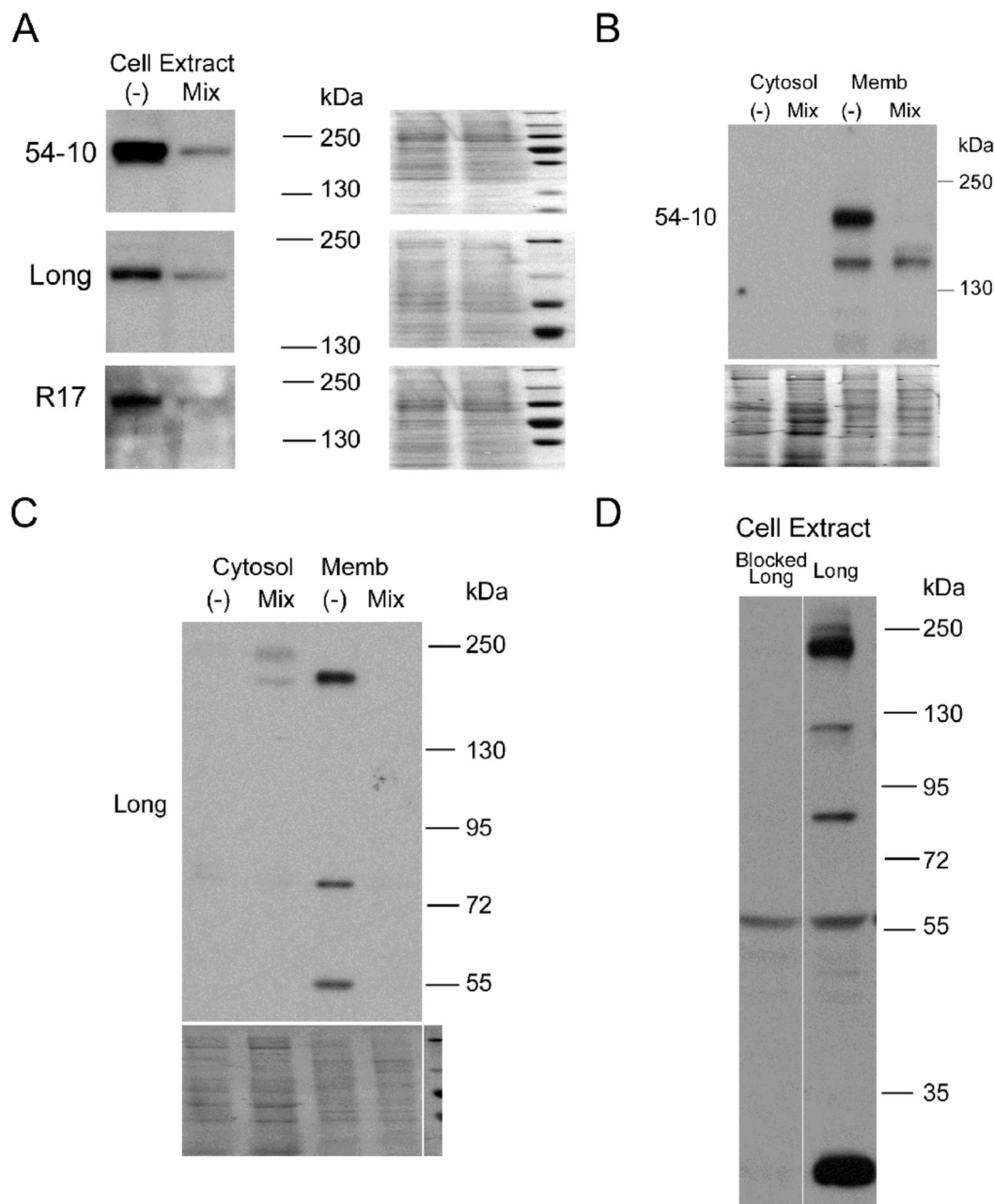
Fig. 4.
Immunoreactive protein expression in Atp7a-specific shRNA expressing ("Mix") or negative control shRNA expressing ("−") IEC-6 cells. Cell extracts were probed with 54–10, Long and R17 Abs (**A**). Cytosol and membrane fractions were probed with 54–10 (**B**) or Long (**C**) Abs. Cytosol is shown to demonstrate the relative purity of the preps. Stained blots in A, B & C exemplify equal protein loading and efficient transfer; **D**. Cell extract was probed with Long or peptide-blocked Long Ab. The line indicates where unrelated lanes were removed from the image. Representative images from several experiments are shown.
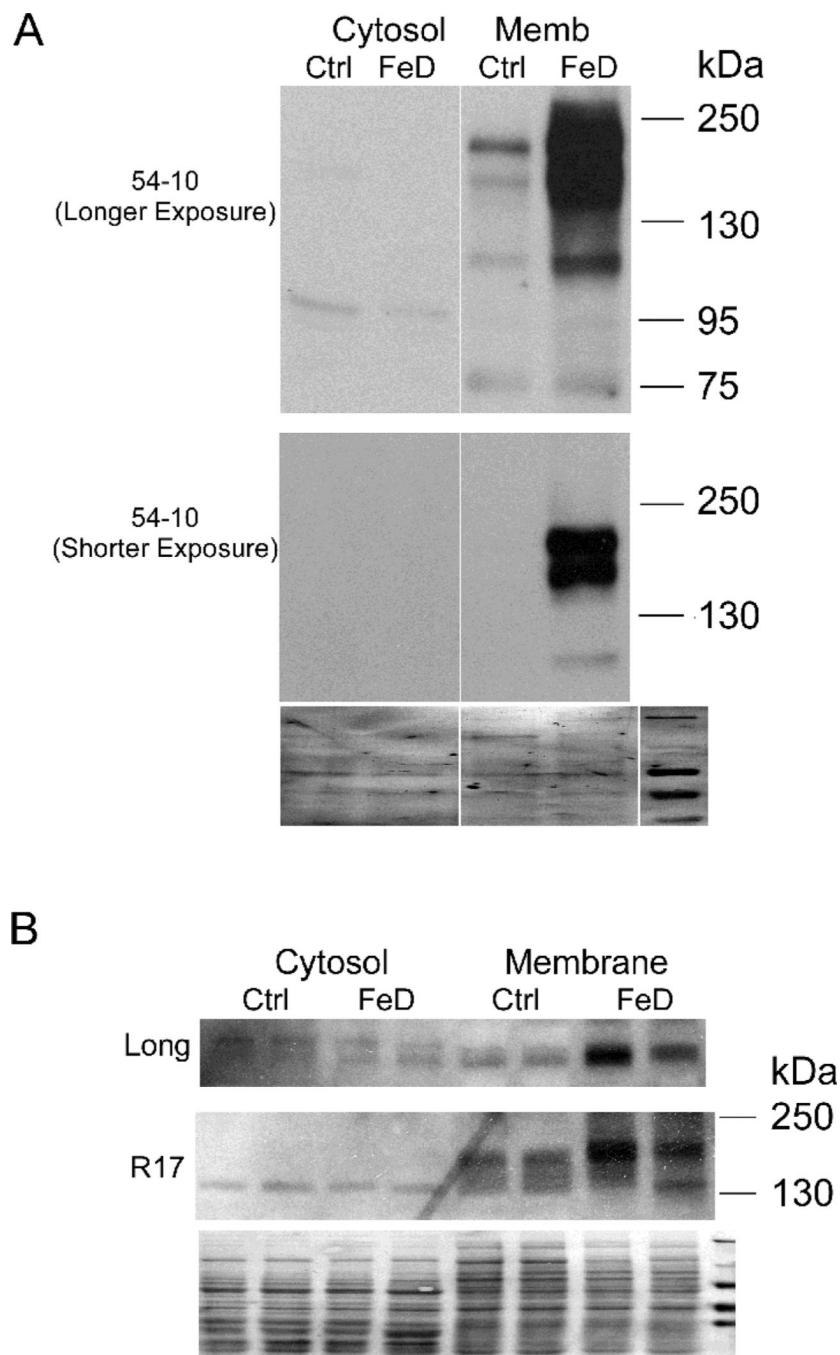
Fig. 5.
Atp7a protein expression in cytosol and membrane fractions of isolated enterocytes from control and iron-deficient (FeD) rat. **A**. Cytosol and membrane fractions were probed with 54–10 Ab. Two different length exposures of the same blot are shown; **B**. Cytosol and membrane fractions were probed with Long and R17 Abs. Stained blots shown in A & B exemplify equal protein loading and efficient transfer. The line in panel A indicates where unrelated lanes were removed from the image. A representative experiment is shown.
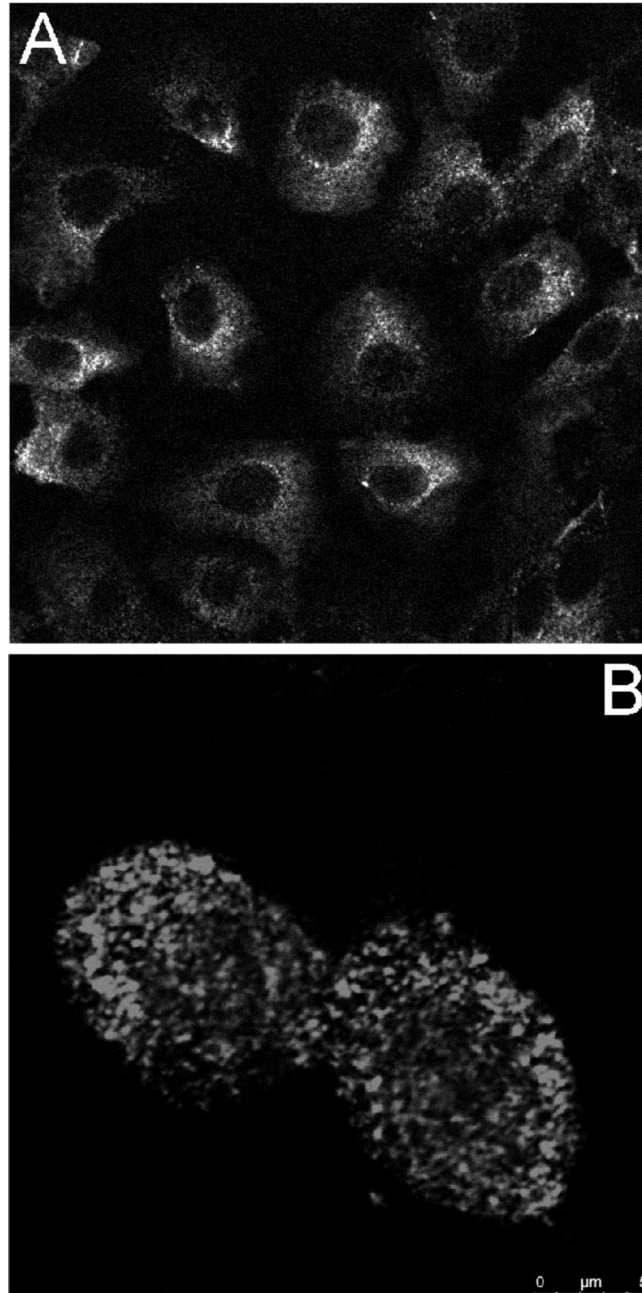
IEC-6 Cells, Long Antiserum

Fig. 6.
Immunocytochemical analysis of IEC-6 cells by Long Ab. **A**. Pre-confluent IEC-6 cells were reacted with Long Ab; **B**. A higher magnification view of IEC-6 cells stained with the Long Ab. A representative experiment is shown.